phosphate behaves as an affinity label and binds with deoxyhemoglobin specifically at the 2,3-DPG (diphosphoglycerate) binding site, allowing the aldehyde function to form a Schiff base with the β NH_2-terminal amino groups (*13*). In order to circumvent the added effects due to electrostatic interactions, only uncharged monosaccharides were included in our experiments.

Our observations may be considered in terms of biomolecular evolution. During the sequential development of anaerobic glycolysis, photosynthesis, and aerobic glycolysis, glucose rather than other stereoisomers has emerged as the universal metabolic fuel. This selectivity could be attributed to the stability of its ring structure, owing to the equatorial orientation of its hydroxyl groups. This stable ring structure greatly retards the rate at which glucose condenses with hemoglobin and, presumably, other proteins and amino-containing compounds (*14*). Conversely, if organisms contained a comparatively high concentration of a metabolic fuel having a relatively unstable ring structure, it is likely that extensive covalent modification of proteins would occur along with potential impairment of function. This prediction is supported by our observations on rats fed a high galactose diet (*5*). (The stability of the ring structure of galactose is one-tenth that of glucose.) The galactosemic rats had more extensive nonenzymatic glycosylation of lens crystallins than did normal rats or even diabetic rats (having elevated blood glucose). Thus, the relatively high stability of its ring structure allows high concentrations of glucose and proteins to coexist in various tissues with a minimal risk of irreversible covalent modification.

H. FRANKLIN BUNN
PAUL J. HIGGINS
Laboratory of the Howard Hughes Medical Institute, Brigham and Women's Hospital, Harvard Medical School, Boston, Massachusetts 02115

References and Notes

1. W. R. Holmquist and W. A. Schroeder, *Biochemistry* **5**, 2489 (1966); R. M. Bookchin and P. M. Gallop, *Biochem. Biophys. Res. Commun.* **32**, 86 (1968); H. F. Bunn, D. N. Haney, K. N. Gabbay, P. M. Gallop, *ibid.* **67**, 103 (1975); R. Flückiger and K. H. Winterhalter, *FEBS Lett.* **71**, 356 (1976); R. J. Koenig, S. H. Blobstein, A. Cerami, *J. Biol. Chem.* **252**, 2992 (1977).
2. H. F. Bunn, D. N. Haney, S. Kamin, K. H. Gabbay, P. M. Gallop, *J. Clin. Invest.* **57**, 1652 (1976).
3. H. F. Bunn *et al.*, *J. Biol. Chem.* **254**, 3892 (1979); R. Shapiro, M. McManus, C. Zalut, H. F. Bunn, *ibid.* **255**, 3120 (1980).
4. V. J. Stevens, C. A. Rouzer, V. M. Monnier, A. Cerami, *Proc. Natl. Acad. Sci. U.S.A.* **75**, 2918 (1978); V. M. Monnier, V. J. Stevens, A. Cerami, *J. Exp. Med.* **150**, 1098 (1979); A. Pande, W. H. Garner, A. Spector, *Biochem. Biophys. Res. Commun.* **89**, 1260 (1979).
5. S.-H. Chiou, L. T. Chylack, H. F. Bunn, J. H. Kinoshita, *Biochem. Biophys. Res. Commun.* **95**, 894 (1980).
6. M. L. Tanzer, R. Fairweather, P. M. Gallop, *Arch. Biochem. Biophys.* **151**, 137 (1972); S. P. Robins and A. J. Bailey, *Biochem. Biophys. Res. Commun.* **48**, 76 (1972); H. Rosenberg, J. B. Mondrak, J. M. Hassing, W. A. Ar-Turk, S. J. Stohs, *ibid.* **91**, 498 (1979).
7. A. J. Bailey, S. P. Robins, M. J. A. Tanner, *Biochim. Biophys. Acta* **434**, 51 (1976); J. A. Miller, E. Gravallese, H. F. Bunn, *J. Clin. Invest.* **65**, 896 (1980).
8. H. F. Bunn, K. H. Gabbay, P. M. Gallop, *Science* **200**, 21 (1978); A. Cerami and R. J. Koenig, *Trends Biochem. Sci.* **3**, 73 (1978).
9. M. J. McDonald, R. Shapiro, M. Bleichman, J. Solway, H. F. Bunn, *J. Biol. Chem.* **253**, 2327 (1978).
10. R. F. Borch, M. D. Bernstein, H. D. Durst, *J. Am. Chem. Soc.* **93**, 2897 (1971); N. Jentoft and D. G. Dearborn, *J. Biol. Chem.* **254**, 4359 (1979).
11. Uniformly labeled D-[^{14}C]glucose and D-[^{14}C]-galactose (New England Nuclear) were purified as described (P. J. Higgins and H. F. Bunn, *J. Biol. Chem.* **256**, 5204 (1981); D-altrose, D-idose, and 5,6-di-*O*-methyl D-glucose were donated by Dr. L. D. Hayward, Vancouver, B.C.
12. L. D. Hayward and S. J. Angyal, *Carbohydr. Res.* **53**, 13 (1977).
13. D. N. Haney and H. F. Bunn, *Proc. Natl. Acad. Sci. U.S.A.* **73**, 3534 (1976).
14. A. Katchalsky and N. Sharon, *Biochim. Biophys. Acta* **10**, 290, (1953).
15. B. Trüeb, C. G. Holenstein, R. W. Fischer, K. H. Winterhalter, *J. Biol. Chem.* **255**, 6717 (1980).
16. Supported by the Howard Hughes Medical Institute and NIH grant AM-18223. We thank Drs. George Cahill, Edmund Lin, and Henry Paulus for helpful discussions.

12 November 1980; revised 27 March 1981

Calcium Dependence of the Inactivation of Calcium Currents in Skeletal Muscle Fibers of an Insect

Abstract. *Calcium currents in skeletal muscle fibers of an insect,* Carausius morosus, *inactivate under depolarization. This inactivation depends on the current being carried across the membrane by calcium ions, rather than strontium or barium ions.*

In many excitable cells, electrical activity is associated with an increase in the permeability of the membrane to calcium ions (*1*). The entry of Ca^{2+}, which occurs as a consequence of membrane depolarization, is important, in excitation-contraction coupling in some muscle fibers (*2*), in excitation-secretion coupling in nerve and secretory cells (*3*), and in the activation of membrane potassium conductance (*4*).

Because Ca^{2+} is involved in the regulation of cellular processes, it is important to know whether entry of Ca^{2+} is maintained during depolarization, as it is in internally perfused muscle fibers (*5*) and certain molluscan neurons (*6*), or whether inactivation occurs and, if so,

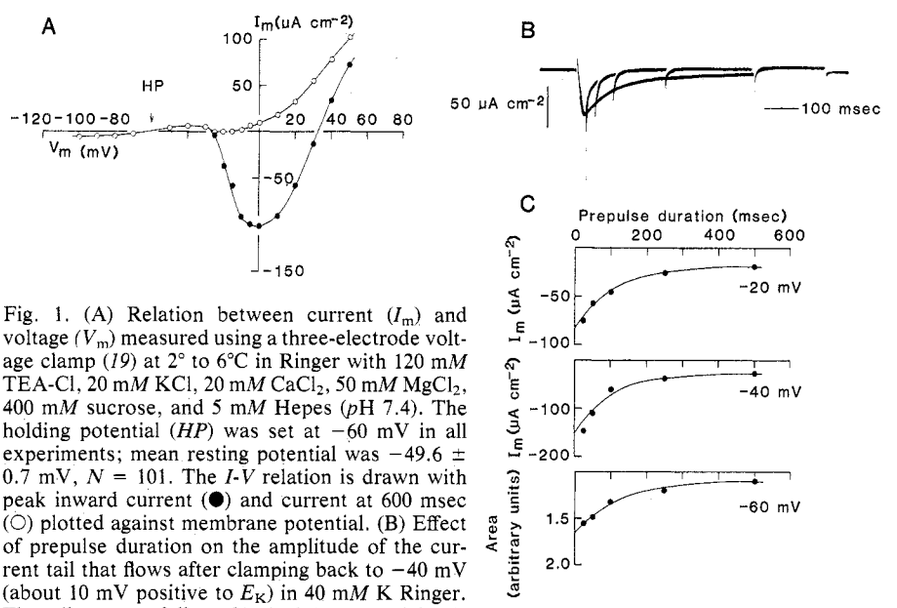

Fig. 1. (A) Relation between current (I_m) and voltage (V_m) measured using a three-electrode voltage clamp (*19*) at 2° to 6°C in Ringer with 120 m*M* TEA-Cl, 20 m*M* KCl, 20 m*M* $CaCl_2$, 50 m*M* $MgCl_2$, 400 m*M* sucrose, and 5 m*M* Hepes (*p*H 7.4). The holding potential (*HP*) was set at −60 mV in all experiments; mean resting potential was −49.6 ± 0.7 mV, N = 101. The *I-V* relation is drawn with peak inward current (●) and current at 600 msec (○) plotted against membrane potential. (B) Effect of prepulse duration on the amplitude of the current tail that flows after clamping back to −40 mV (about 10 mV positive to E_K) in 40 m*M* K Ringer. The tail currents followed a single exponential (τ = 2.64 msec) except during the first few milliseconds, when they were contaminated by capacity transients. The records were superimposed and traced by hand. Resting potential, −33 mV; holding potential, −60 mV; and temperature 4.0°C. (C) Relation between the peak amplitude of the current tail elicited on clamping back to −20, −40 [shown in (B)], or to −60 mV, and the duration of a prepulse to 0 mV. We plotted the area of the transient current at −60 mV, since the current turns off very rapidly at this potential. The curve is drawn to a time constant of 110 msec at −20 mV, 105 msec at −40 mV, and 123 msec at −60 mV. Essentially the same time constant was obtained at −40 mV (τ = 112 msec) by measuring the area of the transient. The Ca current in (B) decayed with a time constant of 105 msec at 0 mV.

0036-8075/81/0710-0224$00.50/0

by what mechanism. In some cells, such as starfish eggs (*7*), inactivation of Ca currents is potential-dependent, somewhat like the inactivation of Na currents is in the squid axon (*8*). But in other cells, such as *Paramecium* (*9*) and neurons of *Aplysia* (*10*), Ca entry appears to be a requirement for inactivation, and little inactivation occurs when Ba^{2+} or Sr^{2+} carry the inward current. We report that the Ca permeability of insect muscle undergoes inactivation and that this inactivation depends on Ca entry. Since the rate of inactivation depends on the permeant ion species, inactivation may be a consequence of an interaction between Ca^{2+} and the Ca channel.

Ventral longitudinal muscles from the third thoracic segment of the stick insect, *Carausius morosus*, were voltage-clamped (*11*) in Ringer containing 120 m*M* tetraethylammonium chloride (TEA-Cl) to block outward K currents and made hypertonic (tonicity twice normal) with sucrose to prevent contraction. Voltage increases to −40 mV (Fig. 1A) elicited a transient inward current which is carried primarily by Ca^{2+} since both the magnitude and apparent reversal potential (*12*) of the current vary appropriately with $[Ca]_o$, and it is blocked by La^{3+} (1 m*M*), Ni^{2+}, and Co^{2+} (10 m*M*) (*11*).

We studied the voltage dependence of the inactivation of the Ca current, using paired pulses separated by a 100-msec interval (Fig. 2A). The interval allowed the activation (as opposed to inactivation) kinetics of the Ca permeability and of any residual K permeability (< 15 percent) to return to their resting state (*13*). The amplitude of the first pulse (pulse 1) was varied and the second, test, pulse (pulse 2) depolarized the membrane to 0 mV, where the Ca current is maximal. After each pulse pair, a single test pulse was used as a control. Figure 2A shows that the peak amplitude of the Ca current during the test pulse depended on the membrane potential during pulse 1 and decreased as this was raised. Inactivation was almost complete when the two pulses were of equal amplitude, but when pulse 1 was further increased the Ca current reappeared during the test pulse.

The voltage dependence of inactivation (Fig. 2C) resembles that of the Ca current (Fig. 1A). There was no inactivation in the absence of a Ca current during pulse 1 and little inactivation when Ca^{2+} entry was small, both at more negative membrane potentials and close to the equilibrium potential for Ca^{2+}. This suggests that entry of Ca^{2+} is required for inactivation of the Ca permeability. We cannot exclude the possibility that a small voltage-dependent component of inactivation also exists, but the presence of some inactivation (about 20 percent) at very positive potentials is consistent with our interpretation, since Ca^{2+} will enter during the current tail that follows repolarization of pulse 1.

We have considered the possibility that the Ca current does not inactivate at all but appears transient because an outward current develops (*1*) or because Ca^{2+} is depleted from some restricted extracellular space (*14*). A potential-dependent outward current cannot account for the decay of the Ca current, since inactivation is reduced at positive potentials. However, a K current activated by Ca entry (*4*) might produce the voltage dependence shown in Fig. 2C. To test this, we returned the membrane to a potential positive to, or negative to, the estimated K equilibrium potential (E_K) (*15*) during the decay of the inward current elicited by a prepulse to 0 mV (Fig. 1, B and C). If the decay of the Ca current was caused by a Ca-activated K current, then an outward current tail, increasing in size with prepulse duration, should occur on clamping back to potentials positive to E_K, and an increasing inward current tail should occur at more negative potentials. At both potentials, however, inward current tails were found, and these decreased with prepulse duration (Fig. 1, B and C) at a rate that was independent of the potential at which they were measured and that was similar to the rate of inactivation of the Ca current elicited by the prepulse. At 0 mV, there is, therefore, little contribution from outward current to the decay of the Ca current.

Figure 2B shows that when Sr^{2+} or Ba^{2+} carry current through the Ca channel, inactivation is slowed and reduced. Since Sr and Ca currents had similar amplitudes (*16*), ion depletion from a

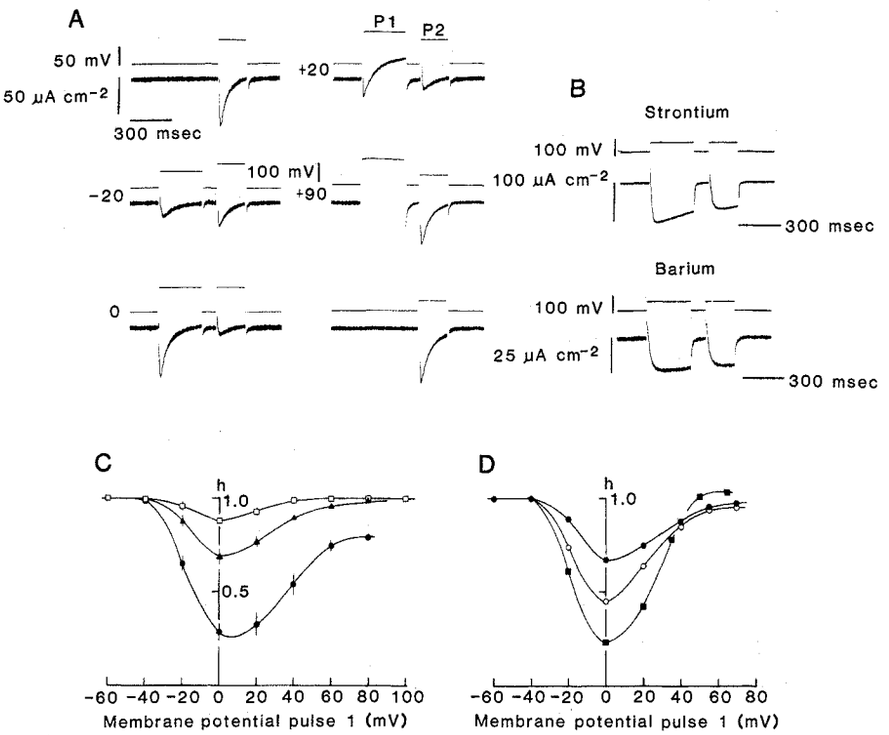

Fig. 2. (A) Effect of varying the amplitude of pulse 1 on the Ca current during pulse 2. The numbers adjacent to each trace indicate the membrane potential during pulse 1. The upper trace is the membrane potential and the lower trace is the membrane current. The voltage gain changed when the amplitude of pulse 1 was +90 mV. Pulse 1: 300 msec; interval 100 msec, −60 mV; pulse 2: 200 msec, 0 mV; RP = −41 mV; HP = −60 mV; and temperature 3°C. (B) Records of membrane potential (top traces) and membrane current (bottom traces) for a pair of voltage pulses to 0 mV, in 20 m*M* Sr Ringer and in 20 m*M* Ba Ringer (*20*). HP = −60 mV; mean RP = −39.8 ± 0.9 mV (N = 9) in Sr Ringer and −46.6 ± 2.5 mV (N = 10) in Ba Ringer. (C) Voltage dependence of inactivation in 20 m*M* Ca (●), Sr (▲), and Ba (□) Ringer. Peak inward current during pulse 2, as a fraction (h) of peak inward current in the absence of a prepulse, is plotted against the membrane potential during pulse 1. Data represent the means and standard errors of three fibers each in Sr and Ba and four fibers in Ca Ringer. Pulse 1: 300 msec; interval 100 msec, −60 mV; pulse 2: 200 msec, 0 mV. (D) Effect of increasing the duration of pulse 1 on the extent of inactivation in Sr Ringer. Pulse 1 duration: 300 msec (●), 800 msec (○), and 3.5 seconds (■); interval 100 msec, −60 mV; pulse 2: 200 msec, 0 mV. The amplitude of pulse 1 is plotted against the peak inward current during pulse 2 as a fraction (h) of that in the absence of a prepulse.

restricted extracellular space, or accumulation inside the fiber, cannot be responsible for inactivation of the inward current. Depletion, or accumulation, would depend on current size, not on the ion species.

The slowing of inactivation in both Sr^{2+} and Ba^{2+} Ringer was accompanied by a marked prolongation of action potentials in these solutions (*17*), emphasizing that the kinetics of the Ca channel are influenced by the permeant ion. We also found a similar, though much less marked, effect on the activation kinetics of the channel: inward currents turned on faster (Fig. 2, A and B) and the inward current tails turned off faster (*18*) in Ca^{2+} than they did in Ba^{2+}.

Our experiments show that steady-state inactivation of the Ca permeability has a voltage dependence similar to that of the inward current and that the rate of inactivation is, at least partly, dependent on the permeant ion. This is in marked contrast to the Na channel of nerve fibers, where the species of the permeant ion does not significantly affect the kinetics of activation and inactivation. Our findings suggest that inactivation of the Ca permeability in insect muscle, as in *Paramecium* and *Aplysia* neurons, is caused by an interaction of the permeant ion with the channel, the ion having to traverse the membrane to produce inactivation. We do not know whether permeant ions bind to a site at the inner membrane surface to produce inactivation or if they influence inactivation during their passage through the membrane by interaction with a site in the Ca channel.

FRANCES M. ASHCROFT*
P. R. STANFIELD
Department of Physiology,
University of Leicester,
Leicester LE1 7RH, United Kingdom

References and Notes

1. S. Hagiwara and L. Byerly, *Annu. Rev. Neurosci.* **4**, 69 (1981).
2. S. Hagiwara *et al.*, *J. Physiol. (London)* **219**, 233 (1971); J. Hildalgo, M. Luxoro, E. Rojas, *ibid.* **288**, 313 (1979).
3. B. Katz and R. Miledi, *ibid.* **203**, 459 (1969); P. F. Baker and T. J. Rink, *ibid.* **253**, 593 (1975).
4. R. W. Meech and N. B. Standen, *ibid.* **249**, 211 (1975).
5. R. D. Keynes, E. Rojas, R. E. Taylor, J. Vergara, *ibid.* **229**, 409 (1973).
6. J. A. Connor, *ibid.* **286**, 41 (1979).
7. S. Hagiwara, S. Ozawa, O. Sand, *J. Gen. Physiol.* **65**, 617 (1975).
8. A. L. Hodgkin and A. F. Huxley, *J. Physiol. (London)*, **116**, 497 (1952).
9. P. Brehm and R. Eckert, *Science* **202**, 1203 (1978).
10. D. Tillotson, *Proc. Natl. Acad. Sci. U.S.A.* **76**, 1497 (1979).
11. F. M. Ashcroft, N. B. Standen, P. R. Stanfield, *J. Physiol. (London)* **291**, 51 (1979).
12. The apparent reversal potential refers to the potential at which the membrane current reverses in sign and is considerably more negative than the Ca equilibrium potential (E_{Ca}) because of contamination by leakage and residual outward currents.
13. H. Meves, *Prog. Biophys. Mol. Biol.* **33**, 207 (1978).
14. W. Almers, R. Fink, P. T. Palade, *J. Physiol. (London)* **312**, 177 (1981).
15. E_K was raised to around −50 mV in these experiments by increasing $[K]_o$ to 40 m*M* because of the rapid decay of the current tails at more negative potentials. In this Ringer, $[K]_i$ measured with intracellular K-selective microelectrodes (ion-exchange resin, Corning 477317) had a mean value of 297.9 ± 3.9 m*M* (111 fibers, eight muscles) at 20°C, giving an E_K of −50.3 ± 0.3 mV.
16. Peak inward current in Ca Ringer was −112.5 ± 14.4 μA cm^{-2} (*N* = 14) and −96.05 ± 13.2 μA cm^{-2} (*N* = 6) in Sr Ringer.
17. Mean action potential duration in Ca^{2+} was 0.35 ± 0.05 second (*N* = nine fibers), 4.1 ± 0.4 seconds (*N* = 11) in Sr^{2+}, and 147 ± 58.1 seconds (*N* = 6) in Ba^{2+}.
18. Decay of inward current tails followed a single exponential with a time constant of 2.64 msec in Ca Ringer and of 5.55 msec in Ba Ringer at −40 mV.
19. R. H. Adrian, W. K. Chandler, A. L. Hodgkin, *J. Physiol. (London)* **208**, 607 (1970).
20. The peak Sr and Ba, but not Ca, currents during pulse 2 were smaller than the current at the end of pulse 1 (see Fig. 2, A and B). This does not imply that inactivation continues during the interval in Ba^{2+} and Sr^{2+} solutions. Hodgkin-Huxley theory [A. L. Hodgkin and A. F. Huxley, *J. Physiol. (London)* **117**, 500 (1952)] predicts that if inactivation does not fully recover during the interval, then by the time the inward current has reached its peak during pulse 2, inactivation may have declined to a lower level than at the end of pulse 1. The pulse 2 current will therefore be smaller. The effect may not be apparent in Ca^{2+} solution because both activation and recovery from inactivation are faster than in solutions of Ba^{2+} or Sr^{2+}.
21. We thank H. E. Edwards for a gift of K-selective resin and N. B. Standen for reading the manuscript. The intercellular [K] measurements were made by C. A. Leech, whom we thank, in collaboration with F.M.A. The work was supported by the Medical Research Council.
* Present address: Department of Physiology, University of California, Los Angeles 90024.

3 September 1980; revised 8 April 1981

Three Distinct Genes in Human DNA Related to the Transforming Genes of Mammalian Sarcoma Retroviruses

Abstract. *Southern blot hybridization was used to identify human and other vertebrate DNA sequences that were homologous to cloned DNA fragments containing the oncogenic nucleic acid sequences of three different type C mammalian retroviruses (simian sarcoma virus, the Snyder-Theilen strain of feline sarcoma virus, and the Harvey strain of murine sarcoma virus). Each* onc *gene counterpart has a single genetic locus, which probably contains non-*onc *intervening sequences. The human DNA sequences may represent genes important to cell growth or cell differentiation, or both. Their identification and isolation may allow elucidation of their role in these processes and in neoplasias.*

All rapidly transforming retroviruses contain nucleotide sequences specific for transformation (termed *onc* genes) and linked to portions of a helper leukemia virus genome (*1*). The *onc* genes are homologous to subsets of normal host cellular DNA that are well conserved among vertebrates (*1*). The cellular homologs of *onc* genes may play a role in neoplastic transformation. Tumor induction in chickens by the avian leukosis virus (RAV-2) is associated with downstream promotion of a cellular gene (*c-myc*) related to the transforming gene of avian myelocytomatosis virus MC29 (*2, 3*). A similar cellular gene present in two diverse species, the chicken and the cat, was found in the genomes of the Fujinami avian sarcoma virus and two strains of feline sarcoma virus (Snyder-Theilen and Gardner-Arnstein) (*4*). All three of the *onc* gene products have associated protein kinase activity (*5, 6*). The number of cellular genes that could be transduced by retroviruses is probably limited, and it is likely that related genes in diverse species have similar functions and may have a role in cell transformation. It is therefore important to determine whether similar genes are present in humans and to analyze these genes before examining their role in cell growth, differentiation, and tumorigenesis in man.

We used molecularly cloned DNA fragments containing transformation-specific sequences of three mammalian sarcoma retroviruses—the woolly monkey (simian) sarcoma virus (SSV), the Snyder-Theilen strain of feline sarcoma virus ($FeSV_{ST}$), and the Harvey murine sarcoma virus (HaMSV)—to detect homologous DNA sequences in man and lower vertebrates by Southern (*7*) hybridization. These viruses differ from each other in their hosts of origin (primate, cat, and rat, respectively), in the arrangement of their genes, and in the structure of the *onc*-specific protein. Like a number of other acutely transforming retroviruses including Abelson murine leukemia virus (*8*) and the avian viruses MC29 (*9*), avian erythroblastosis virus (*10*), and Fujinami sarcoma virus (*11*), $FeSV_{ST}$ codes for a fused polypeptide containing *gag*- and *onc*-directed peptides and an associated tyrosine protein kinase activity (*12, 13*). The gene order of $FeSV_{ST}$ is 5′-*gag-onc-env-C*-3′ (*gag* and *env* are antigenic determinants of core and envelope proteins, respectively, and *C* is a noncoding region) (*14*). The HaMSV is a double recombinant containing the 5′ and 3′ termini of the

0036-8075/81/0710-0226$00.50/0